

Design and characterization of a compact array of MEMS accelerometers for geotechnical instrumentation

V. Bennett* and T. Abdoun‡

Department of Civil and Environmental Engineering, Rensselaer Polytechnic Institute, 110 8th Street, JEC 4049, Troy, NY 12180, USA

T. Shantz‡†

California Department of Transportation, Division of Research and Innovation, 1227 O Street, MS-83, P.O. Box 942873, Sacramento, CA 94273, USA

D. Jang‡‡

Branch A Geotechnical Design – South 1, California Department of Transportation, Division of Engineering Services, Geotechnical Services, MS 5, 5900 Folsom Boulevard, Sacramento, CA 95819, USA

S. Thevanayagam‡‡†

Department of Civil and Environmental Engineering, University at Buffalo, 133 Ketter Hall, Buffalo, NY 14260, USA

(Received November 10, 2008, Accepted April 27, 2009)

Abstract. The use of Micro-Electro-Mechanical Systems (MEMS) accelerometers in geotechnical instrumentation is relatively new but on the rise. This paper describes a new MEMS-based system for in situ deformation and vibration monitoring. The system has been developed in an effort to combine recent advances in the miniaturization of sensors and electronics with an established wireless infrastructure for on-line geotechnical monitoring. The concept is based on triaxial MEMS accelerometer measurements of static acceleration (angles relative to gravity) and dynamic accelerations. The dynamic acceleration sensitivity range provides signals proportional to vibration during earthquakes or construction activities. This MEMS-based in-place inclinometer system utilizes the measurements to obtain three-dimensional (3D) ground acceleration and permanent deformation profiles up to a depth of one hundred meters. Each sensor array or group of arrays can be connected to a wireless earth station to enable real-time monitoring as well as remote sensor configuration. This paper provides a technical assessment of MEMS-based in-place inclinometer systems for geotechnical instrumentation applications by reviewing the sensor characteristics and providing small- and full-scale laboratory calibration tests. A description and validation of recorded field data from an instrumented unstable slope in California is also presented.

Keywords: autonomous geotechnical monitoring; wireless data transmission; MEMS.

*PhD Student, Corresponding Author, E-mail: bennev@rpi.edu

‡Professor, E-mail: abdout@rpi.edu

‡†Senior Research Engineer, E-mail: tom_shantz@dot.ca.gov

‡‡Chief, E-mail: deh-jeng_jang@dot.ca.gov

‡‡†Professor, E-mail: theva@buffalo.edu

1. Introduction

MEMS-based in-place inclinometer systems use an array of triaxial Micro-Electro-Mechanical Systems (MEMS) accelerometers, housed in short rigid segments, to measure permanent ground deformation and acceleration profiles for geotechnical monitoring. MEMS accelerometers have been used for decades in the automotive industry but have recently become available with ranges of 2 g or less and with drift and resolution specifications equal to or better than earlier technologies. Consequently, these devices have been recently used by geotechnical instrumentation manufacturers for in-place inclinometers, tiltmeters, tilt beams, probe inclinometers and strong-motion accelerographs (Sellers and Taylor 2008). The use of MEMS devices in geotechnical instrumentation has seen a notable increase in recent years, however the use of these devices is fairly well-established in structural health monitoring (Tanner, *et al.* 2003, Lynch, *et al.* 2004, Pakzad and Fenves 2004).

In spite of the growing awareness of the importance of accelerometer downhole arrays (Elgamal, *et al.* 1995, Zeghal, *et al.* 1995, Elgamal, *et al.* 1996), particularly when combined with pore pressure sensors and inclinometers to capture information on soil liquefaction and lateral spreading (Youd and Holzer 1994, Zeghal and Elgamal 1994), these arrays still remain scarce. The recent advances in sensors and wireless networking technologies have made it possible to capture in situ measurements with much higher sensor density and allow for more continuous access to data, enabling better understanding of soil and soil-structure systems exposed to natural forces or construction activities (Hoffman, *et al.* 2006). The wireless ShapeAccelArray (SAA) sensor (Danisch, *et al.* 2004), manufactured by Measurand Inc., presented in this paper is an example of recent advances in sensors and wireless networking technologies applied to geotechnical instrumentation.

Unlike collections of tilt sensors that bend in a single direction, the wireless ShapeAccelArray (SAA) is a flexible, calibrated and water-tight three-dimensional (3D) measuring system requiring no other fixturing guides. The SAA bends freely, without a preferred axis, in three degrees of freedom. This sensor array employs Micro-Electro-Mechanical systems (MEMS), which have enabled gravity-based three-dimensional (3D) displacement calculation. SAA uses MEMS accelerometers in a pre-calibrated, geometrically constrained array (Danisch, *et al.* 2004) to provide long-term stability previously unattainable with fiber optic methods and calculate 3D polylines representing the complete sensor array 3D profile. The use of accelerometers also provides a ready means of in situ vibration measurement along the array. This sensor array is thus capable of measuring 3D soil acceleration and 3D permanent ground deformations up to a depth of one hundred meters. While the sensor array can be constructed to greater lengths, it has only been verified to be watertight up to 100 m. Similar to all instrumentation scenarios, this MEMS-based system also has technical limitations that will be discussed in this paper.

This paper provides an assessment of MEMS-based in-place inclinometer systems for geotechnical instrumentation applications by reviewing the sensor characteristics and providing small- and full-scale laboratory calibration tests. A description and validation of recorded field data from an instrumented slope will also be presented. MEMS measurements are compared with independent, direct measurements of the ground deformations and accelerations. The time-dependent characteristics of this system are qualified through long-term, i.e. more than two years of, monitoring.

2. Description of MEMS-based in-place sensor array

The wireless ShapeAccelArray (SAA) sensor, manufactured by Measurand, Inc., was used in this study.



Fig. 1 Photograph of the wireless ShapeAccelArray and corresponding visualization of sensor positions

Measurand ShapeTape (Danisch 1998) uses fiber optic sensors to measure curvature, and algorithms to calculate 3D, six-degree-of-freedom displacement profiles (Danisch, *et al.* 2003). The wireless ShapeAccelArray provides similar calculations, using MEMS technology (manufactured by Analog Devices) to provide reliable long-term stability for static measurements and high-speed vibration for dynamic cases. Fig. 1 shows a photograph of an SAA and the corresponding visualization of the sensor positions. The SAA is a segmented array, flexible in two degrees of freedom between 0.305 m long rigid segments, with a maximum instrument diameter of 25 mm and a length up to 100 m. The SAA is designed to be capable of measuring 3D soil permanent deformation and 3D accelerations, provide high resolution measurement in time (sampling rate higher than 70 Hz for dynamic measurement) and space (locations between measurements can be as close as 0.25 m), and contain modular components to enable variable sensor spacing and multiplexing. Two slightly different versions of the SAA were developed, with wireless acquisition for in situ (field) installation or with enhanced acquisition bandwidth and high sampling rate for laboratory research installations. The in situ monitoring system is designed to be placed in a borehole for monitoring active slopes, reinforced earth structures, mines and urban excavations, etc.

The MEMS accelerometers mounted in pipes on a mechanical goniometer (a device that allows the pipe to be rotated to a precise angular position) readout have an estimated absolute accuracy similar to that of conventional inclinometers and excellent 'linearity' over a 45 degree range from their initial position. 'Linearity' is the match of the arcsine of the output to the tilt in degrees since MEMS accelerometers exhibit a sinusoidal response to tilt (output voltage = $\sin(\text{angle})$). Accuracy of the SAA system, similar to traditional probe inclinometers, is best near either pure vertical or pure horizontal (probe inclinometers are usually specified within ± 3 degrees of vertical). In the case of MEMS accelerometers, the sinusoidal

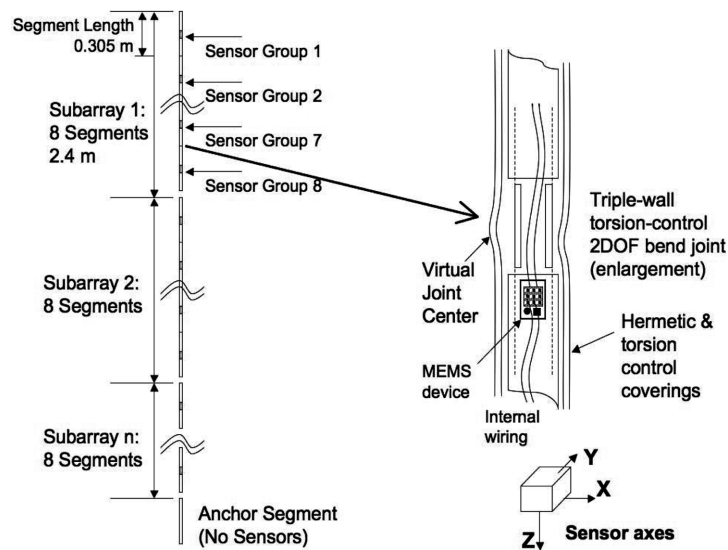


Fig. 2 Schematic drawing of vertical field version of the wireless ShapeAccelArray

response causes a very gradual degradation away from the set initial position, due to a decrease in slope of the sinusoid away from its “zero-crossing”. At ± 10 degrees from vertical, the sine curve slope is degraded by only 1.5 percent, and at ± 45 degrees is degraded by only 29 percent. That is, the MEMS accelerometers remain accurate even when the array is deformed to significant angles from vertical. Similar numbers apply to deviation from a horizontal position, due to the use of three MEMS accelerometers per segment.

A microprocessor and other circuitry on a small printed circuit board (PCB) are built into the array, at intervals of eight segments. The microprocessor services the triaxial MEMS (Fig. 2). 3D orientation is derived from the MEMS readings along the substrate using 3D transforms, as described in the next section, and the built-in geometric constraints of the joints. Dynamic acceleration is measured in the horizontal plane at multiple points to provide signature data for earthquakes.

The SAA system is built in subarrays, as presented in Fig. 2. A subarray is a contiguous grouping of eight 0.305 m rigid segments (in the standard design), with a microprocessor that collects data from triaxial MEMS accelerometers in each segment. This design enables calibration of a subarray individually prior to concatenation of subarrays into a full sensor array of a length determined by the end user. A calibration subroutine allows adjustment of the torsional offsets between subarrays during concatenation. When fully assembled, the array is already calibrated to measure in situ 3D permanent ground deformation at 0.30 m intervals and 3D soil acceleration at 2.4 m intervals. High flexibility and high sensor density result in enhanced spatial resolution along the array and the ability to capture even significantly distorted displacement profiles. Torsional constraint, and 3D pre-calibration of the complete SAA, eliminates the need for torsional alignment systems, such as grooved borehole casings, which are typically used with traditional probe and in-place inclinometer systems.

A full temperature calibration is done on each MEMS sensor individually prior to its inclusion in an array. Measurand has completed a study of the temperature coefficients of the MEMS accelerometers and concluded that the change in output of the sensor is linear with temperature. Calibration files associated with each SAA allow the automatic correction for temperature effects in each individual sensor. A digital

temperature sensor is included within the SAA near each microprocessor. Thus, each temperature sensor calibrates the MEMS sensors in the eight segments surrounding it. This configuration is deemed sufficient for typical underground applications as the ground temperature is usually constant below 1.5 m from the surface. A denser construction of temperature sensors would be possible but only necessary if a large temperature gradient is expected across any consecutive eight segments, or if the temperature gradient is in a location where ground deformations are expected. The standard operating and storage temperature of the SAA is -20° to 70°C .

Each sensor array in the field is connected to a wireless earth station to enable real-time monitoring of a wide range of soil and soil-structure systems as well as remote sensor configuration. The earth station for the array includes a small computer with embedded firmware. This computer runs autonomously, communicating with the array and uploading data wirelessly at prescribed intervals by File Transfer Protocol (FTP). Instructions for the system are placed on the FTP server by an administrator or by another autonomous program. These instructions are used to change collection times, alarm limits, upload times, and other configuration parameters.

3. Method of displacement calculation

The ShapeAccelArray measures displacement, expressed as a series of positions in x , y , and z directions and a set of orientations associated with these points. The positions form a 'polyline'; in other words, the positions describe a series of line segments connected at vertices. The orientations are expressed as sets of unit orientation vectors, which may be converted to Euler angles or quaternions (Danisch 1998). A polyline may be created by performing rotations on its line segments. In the general case, the polyline may represent connected objects that can be bent in two degrees of freedom and twisted in one degree of freedom. If the bends and twists are known, the polyline may be calculated by the following geometrical rotation process. The position of a rigid segment, S , may be described in an X , Y , Z world coordinate system as $(X1, Y1, Z1)$ relative to the origin $(0, 0, 0)$. The orientation of S may be described by a set of mutually orthogonal unit vectors N , B , U in the world coordinate system. In the simplest case, N , B and U are aligned with X , Y , and Z , as shown in Fig. 3. In order to transform this simplest case to a more general case, a segment can be rotated within its local coordinate system (i, j, k) in three degrees of freedom (two

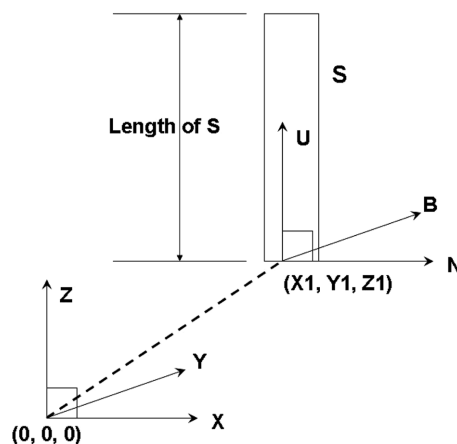


Fig. 3 Three-dimensional description of a segment of the ShapeAccelArray

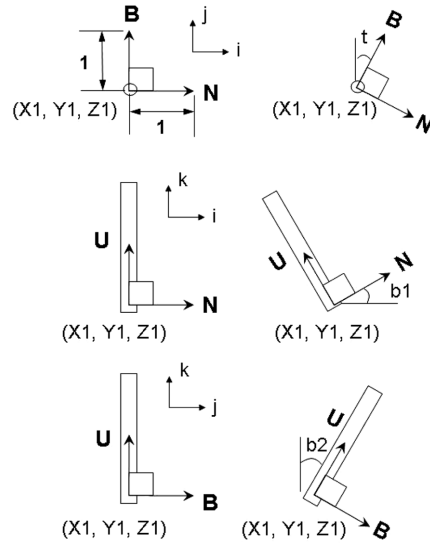


Fig. 4 Degrees of freedom rotations of one segment of the ShapeAccelArray

bends and one twist). The following figures illustrate the general utilization of the measurements from MEMS devices for the reported displacements of an SAA. These algorithms are included in the SAA software.

Fig. 4 shows the following series of axes rotations: B and N are rotated about U through a torsional angle, t ; U and N are rotated about B through a first bend angle, $b1$; and U and B are rotated about N by a second bend angle, $b2$. The center of the line segment S is now completely defined by the vectors X1, Y1, Z1 and N, B, U and the known length of the line segment.

Through this same set of operations, a previously aligned set of segments, see segments S1, S2, S3 and S4 in Fig. 5, can be transformed to an arbitrary positions by performing a series of rotations by the torsional angle, t , and bend angles, $b1$ and $b2$, of each segment relative to the preceding segment. The

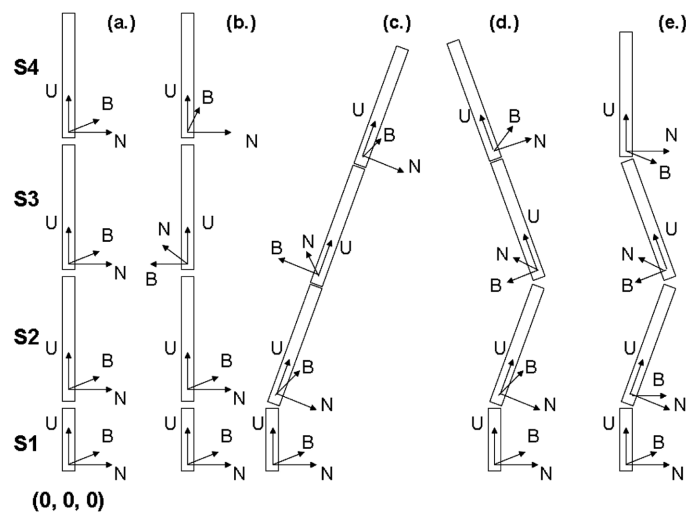


Fig. 5 Transformation of segments into an arbitrary displacement profile by a series of rotations and bends

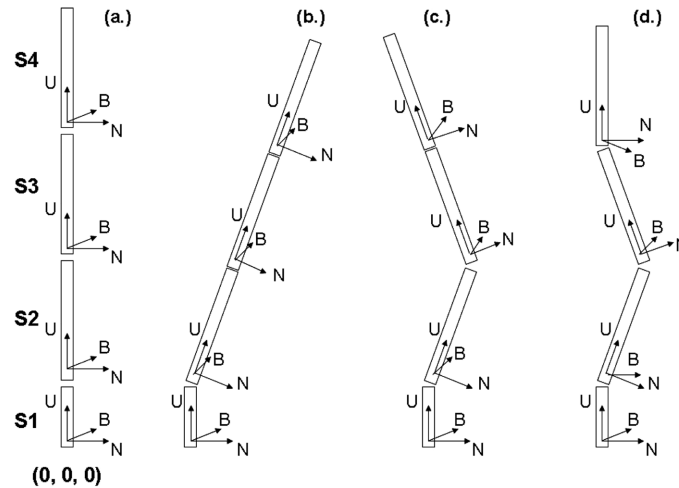


Fig. 6 3D polyline with the same displacement profile as a physical ShapeAccelArray resulting from a series of orientations determined from virtually aligned accelerometer tilt values

segments, S1 through S4, are originally aligned, as seen in Fig. 5(a). Segments S1 through S4 are then rotated by torsional angles, t 's, to obtain the orientation in Fig. 5(b). Segments S2 through S4 then experience a combination of bends, $b1$ and $b2$, to obtain arbitrary three-dimensional positions, Fig. 5(c-e). Since the rotations are relative to preceding segments, torsional angles, t 's, may be thought of as twists, and $b1$'s and $b2$'s as bends.

Triaxial accelerometers are used to sense the x and y components of the gravity vector in each segment. During manufacture, the accelerometers are not aligned torsionally within the segments, but are at known torsional angles, t 's, determined after construction. SAA joints are physically constrained not to twist, so the calibration t 's may be used to align the sensor readings torsionally. The aligned x and y components of the gravity vector represent absolute tilt angles, T 's, in the world coordinate system. To determine the three dimensional displacement profile of the array, the measured x and y components are rotated by the known torsional angles to find a new set of aligned tilt components. After the alignment process using calibrated torsional values, t 's, and after local bends, b 's, are known from the absolute tilts, T 's, the position profile of the SAA can be calculated. This calculation is the same as described in Fig. 5, without any twist stage, that is, two degrees of freedom bend only. The physical segment lengths are specified in a factory calibration file and are used to scale each segment of the calculated 3D polyline. The segments S1 through S4 are virtually aligned to an initial position in Fig. 6(a), then through a series of orientations determined from the accelerometer tilt values (i.e., deviations from the initial position), the result is a 3D polyline with the same position profile as the physical array, see Fig. 6(b-d). Because the joints are torsion-constrained, the two tilt components per segment are sufficient to calculate a 3D rotational transform between each pair of segments. There is no limitation on the displacement profile that can be calculated, as long as no portion is horizontal. The displacement profile is truly 3D, with x, y, and z being known for all parts of the array.

4. Laboratory sensor calibration tests

In an effort to verify the SAA measured displacement and acceleration, these measurements were

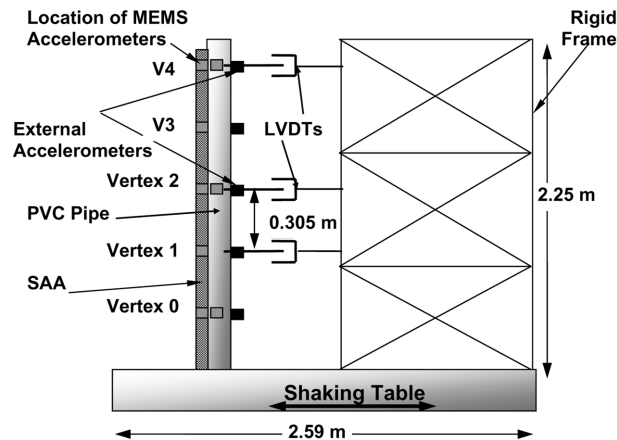


Fig. 7 Setup for testing the ShapeAccelArray on RPI's 1 g shaking table

compared to those from established methods. A series of calibration tests using the 1g seismic shaking table facility at Rensselaer Polytechnic Institute (RPI) were conducted. RPI's seismic shaking table has a 2.59 m by 1.63 m platform area with an available payload capacity of approximately 45 kN. The table setup performs up to a maximum acceleration, velocity, and displacement of 5 g, 30 cm/s, and ± 13 cm, respectively. A servo-controlled hydraulic actuator drives the table and is controlled by a closed-loop proportional integral derivative filter (PIDF) controller that utilizes the actuator displacement as the feedback signal, allowing for the accurate use of very complex input motion (Reigles 2005). Due to the preliminary nature of this testing, simple sinusoidal functions were used as the input motion for this series of calibration tests.

Fig. 7 presents a schematic of the shaking table test setup. A 1.5 m long sensor array, which included four sensing elements placed at 0.305 m intervals, built with local multiplexing (PIC microprocessor with RS485 communication) to facilitate faster sampling and noise reduction, was attached to a flexible and rigid pipe, respectively, and the bottom of this assembly was fixed to the table platform. The flexible pipe was used to simulate large acceleration with large relative displacement, while the rigid pipe simulated large accelerations with minimal relative displacement. Both of these situations can be expected in the field depending on local soil conditions, i.e. stiff and/or loose clays and sands. The response of the setup was also monitored using traditional variable capacitance accelerometers and analog magnetostrictive position sensors. One accelerometer and one position sensor was attached to each of the four instrumented vertices of the SAA. A reference accelerometer was also included on the shaking table surface to capture

Table 1 Input frequency and amplitude combinations for shaking table calibration tests

PVC Setup		ALUM Setup	
Freq (Hz)	Accel Amp (g)	Freq (Hz)	Accel Amp (g)
0.5	0.08	0.5	0.08
1	0.1	1	0.15
1.5	0.3	1.5	0.4
2	0.5	2	0.6
2.5	0.6	2.5	0.6
2.5	1.4	2.5	1.2

the actual input motion. The test setup was excited by different combinations of acceleration amplitudes and frequencies, ranging from 0.08 g to 1.4 g and 0.5 Hz to 2.5 Hz, respectively, see Table 1 for all experimental combinations. In every combination, a very close comparison of SAA and reference sensor measurements was observed.

Fig. 8 presents a comparison between acceleration time histories, in response to a 0.5 Hz excitation frequency, recorded using the SAA and external accelerometers located at vertices one (bottom of the assembly) through four (top of the assembly), for the flexible pipe assembly. The acceleration of the table

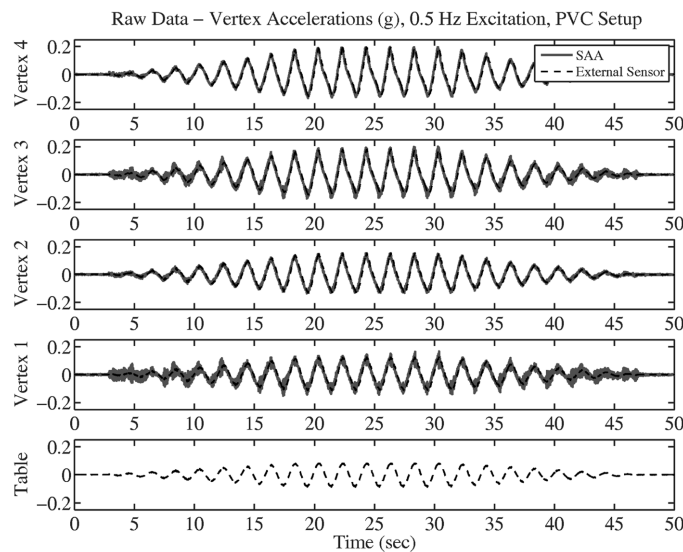


Fig. 8 Comparison between acceleration (g) measured using traditional accelerometers and the ShapeAccelArray on a flexible assembly, at 0.5 Hz excitation frequency

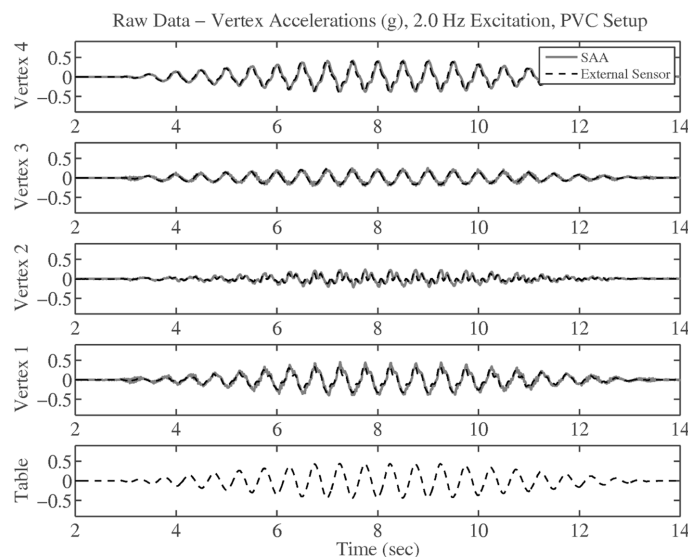


Fig. 9 Comparison between acceleration (g) measured using traditional accelerometers and the ShapeAccelArray on a flexible assembly, at 2.0 Hz excitation frequency

surface is also included at the bottom of the plot, for comparison. The reference accelerometers were filtered, by default setting, above 10 Hz, while the MEMS accelerometers were not filtered at all. Thus, some high frequency noise can be observed in the SAA measurements. A similar plot is presented in Fig. 9, which is an acceleration time history comparison in response to a 2.0 Hz excitation frequency. A very close comparison is again observed at this input frequency. The aluminum pipe setup was used to simulate large acceleration with minimal relative displacement. Experiments on this setup roughly simulate a very

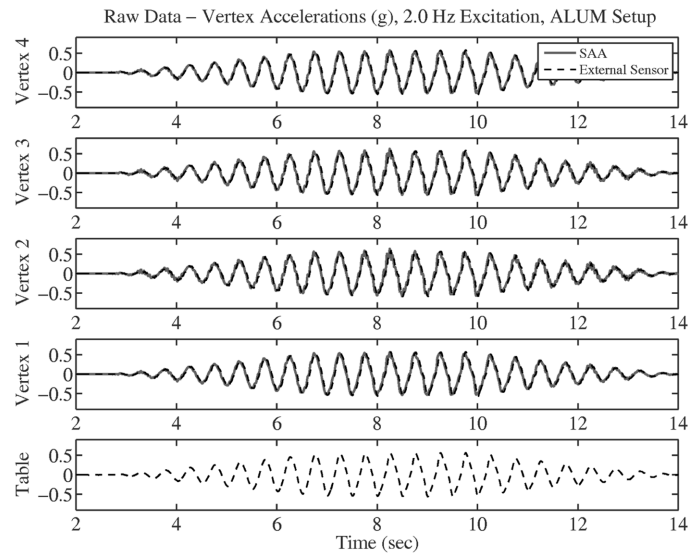


Fig. 10 Comparison between acceleration (g) measured using traditional accelerometers and the ShapeAccelArray on a rigid assembly, at 2.0 Hz excitation frequency

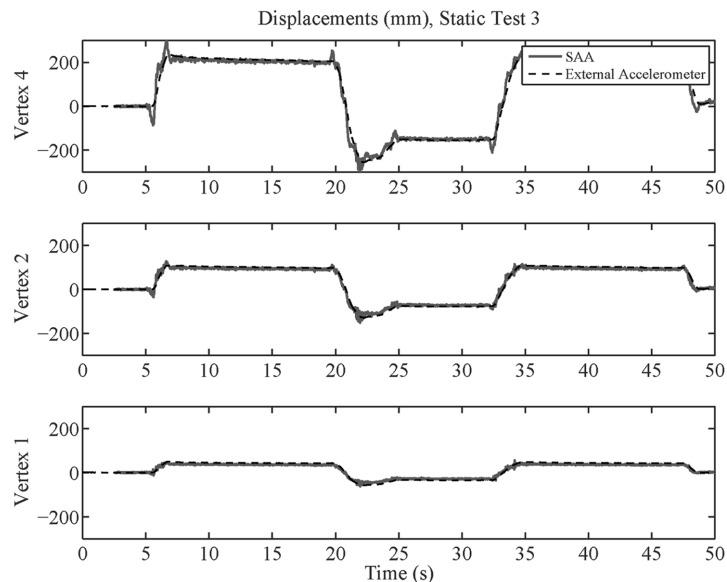


Fig. 11 Comparison between static lateral displacements (mm) measured using traditional position sensors and the ShapeAccelArray

dense soil deposit. Fig. 10 shows an acceleration time history comparison in response to a 2.0 Hz excitation frequency for the aluminum pipe setup. These comparison results seem to indicate that the SAA sensor array is applicable to field installations, where a varying range of ground shaking frequencies can be expected.

In order to simulate the case of typical landslide displacement, the SAA, on the flexible pipe assembly, was displaced and held in static poses for brief intervals of time. Fig. 11 presents a comparison between these permanent lateral deformations measured using the sensor array and a reference position sensor, located at vertices one, two and four. As in the case of acceleration, this figure shows a very good comparison between the measurements of the traditional displacement sensors and the sensor array. For further information on this test, please see Abdoun, *et al.* (2006).

5. Full-scale validation tests

Full-scale calibration tests were conducted with SAAs in order to validate the sensor measurements within a sloping soil deposit subjected to base acceleration. Researchers at the University at Buffalo (UB) and Rensselaer Polytechnic Institute (RPI) developed a large-scale earthquake simulator to model the response of saturated sand to earthquake forces. The earthquake simulator is part of the NEES@Buffalo equipment and research site, a National Science Foundation (NSF) facility. A main component of this simulator is the laminar container at the University at Buffalo, which is 5 m long, 2.75 m wide and 6 m high and is capable of containing 150 tons of saturated sand. Specially designed ball bearings are used between each of the 0.254 m thick laminates to achieve nearly frictionless sliding (Fig. 12(a)). After filling the container, which was inclined at 2 degrees, with loose sand and water, two 100-ton hydraulic actuators were used to impart pre-determined motion to the base of the box. The resultant soil liquefaction and lateral spreading was monitored using variable capacitance accelerometers within the deposit and on the laminates, potentiometers (displacement sensors) on the laminates, pore-pressure transducers and two SAAs within the soil deposit. The results from one of the two 7 m long SAAs installed in a sloping ground test will be presented herein. Each of these sensor arrays contained 24 3D sensing elements. One SAA was placed in the center of the laminar container and a second array was 1 m upstream of the center, along the centerline of the container (Fig. 12(b)). Arrays were fixed at the bottom of the container with a two-

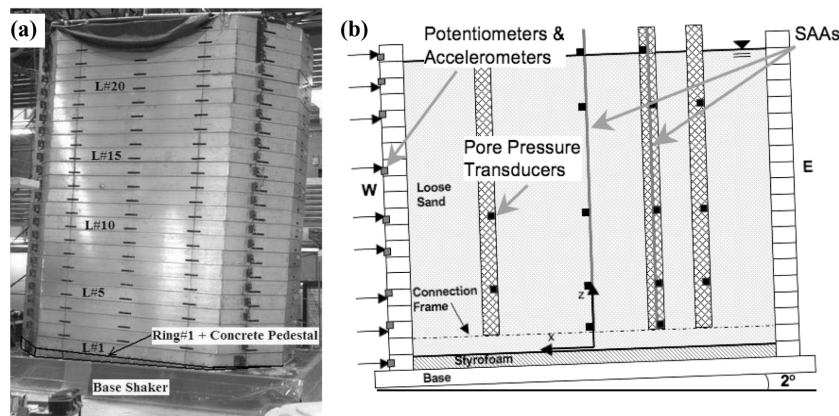


Fig. 12(a) Photo of inclined laminar container; (b) Layout of instrumentation within NEES@Buffalo full-scale laminar container and on laminates

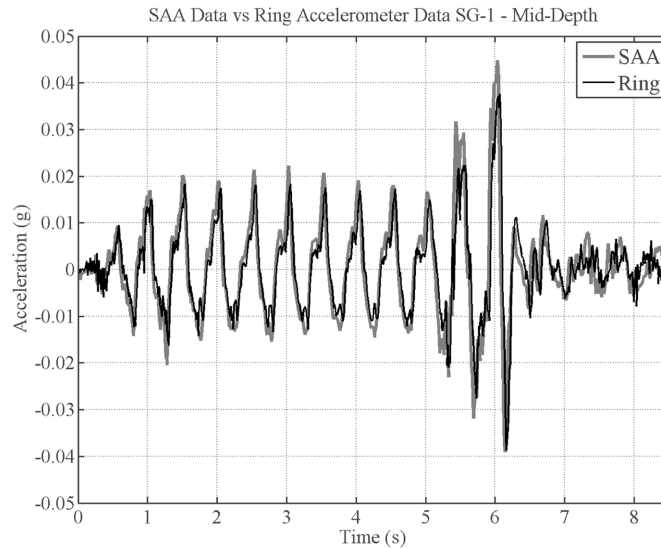


Fig. 13 Acceleration measurement comparison between SAA and accelerometer on the laminar ring at mid-height of the laminar container

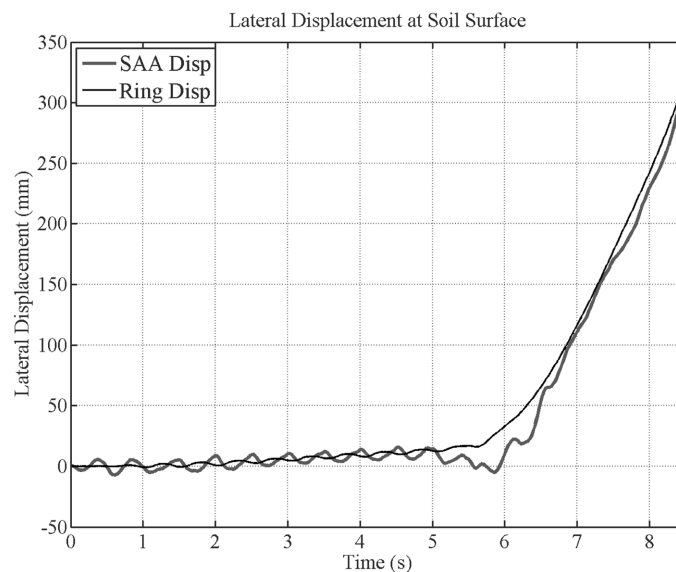


Fig. 14 Lateral displacement comparison between SAA and potentiometer on the container ring at the soil surface

point clamp to provide a reference end and were installed prior to the soil placement.

The 5 m soil model was subjected to input motion that induced 30 cm of permanent lateral displacement at the ground surface after 8.5 s of shaking. Fig. 13 presents a comparison between acceleration time histories recorded using the center SAA and the traditional accelerometers located on the laminates. Displacement readings from potentiometers were only available for the outside of the laminar box as these displacement gages were fixed to the laminates. It is expected that the soil movement will match that of the laminates at the soil surface, thus a permanent displacement comparison is included of that location. Fig. 14 presents a comparison between permanent lateral deformation time histories measured using the

center SAA and the potentiometer on the uppermost laminate. The SAA was not designed to record dynamic cyclic lateral displacements, thus the SAA data was filtered above 1Hz to obtain this permanent displacement trend. Around 6 s, the SAA data deviates slightly from the potentiometer data, which can likely be attributed to the effect of filtering the dynamic displacement. The lateral spreading of the soil deposit initiated around this time, indicating a limitation to this type of instrumentation, i.e., the inability to capture detailed displacements at the narrow time frame of lateral spreading initiation. Similar comparison results were obtained at different soil elevations with the downstream and upstream sensor arrays.

6. In situ sensor validation tests

To validate the acceleration and displacement measurements collected by the SAA in field applications, this system was installed at two locations in California and several in upstate New York. “Site A” in California, described below, was utilized for landslide and lateral spread monitoring of an unstable slope. According to Caltrans’ geotechnical site reports, the slope is part of an older and larger landslide prone area. The affected area is approximately 225 m long and 66 m to 100 m wide. Cracks of the highway pavement were first observed in February 2005 and since then a series of curvilinear cracks have developed at the top of the slope, primarily in Lane No. 2 of the eastbound highway. Further investigation revealed that a distinct curvilinear scarp had formed and a maximum differential settlement of about 50 mm across the scarp was measured. From 2002 to 2005, four traditional inclinometer casings were installed at the highway level (Fig. 15). This collection of instrumentation allowed for comparative analysis between the traditional inclinometer values and those from the SAA. The SAA system was installed approximately one meter away from a newly installed traditional inclinometer casing.

The “Site A” SAA was 19.52 m long, which enabled embedment into a known stable soil layer (Fig. 16). This stable soil layer below 14 m depth was identified by Caltrans’ geotechnical site reports dating back to 2002. Threaded 3.05 m long, 76.2 mm inner diameter PVC casing sections were used in a 127 mm

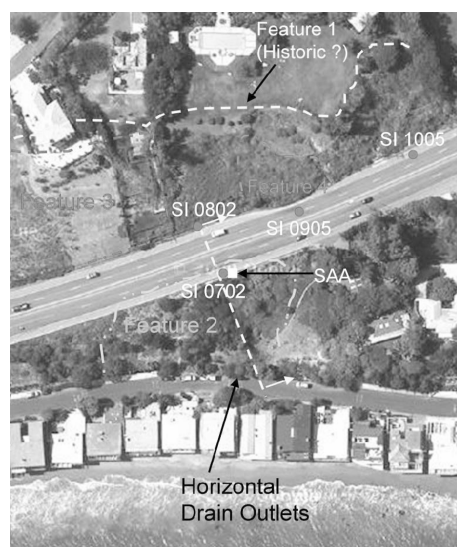


Fig. 15 Aerial photo of “Site A,” California with locations of four slope inclinometer casings. (Photo courtesy Caltrans)

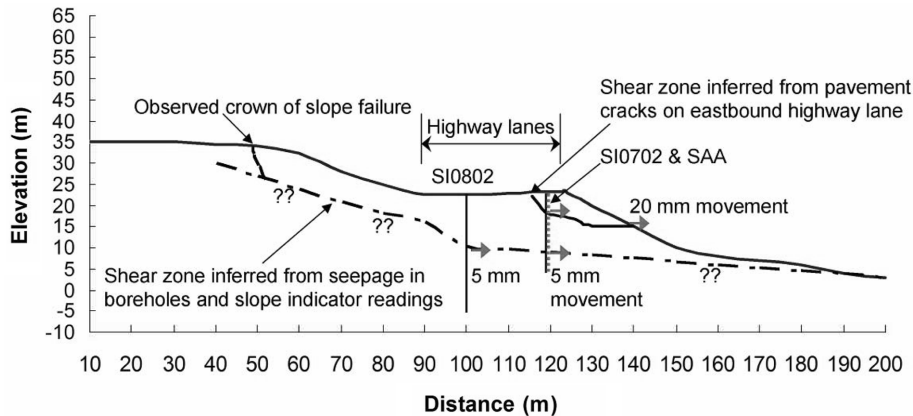


Fig. 16 Cross section of unstable slope, “Site A”, California. (Figure courtesy Caltrans)

diameter borehole. To couple the SAA to the PVC casing, coarse sand was poured from the top of each casing section as the sections were attached (Abdoun, *et al.* 2007). In order to minimize the potential for the casing backfill to liquefy during an earthquake and compromise the coupling between the sensor and the casing, two precautions were taken. First, in an effort to keep the interior of the casing dry, the PVC casing was installed with a sealed end cap with greased o-rings at each threaded section. Second, in the event water did enter the casing, the sand was densified, to the extent possible, by striking the side of the casing during the placement of the sand. Each section of PVC casing was advanced along the array toward the borehole as the installation progressed. The sensor array can be retrieved, upon completion of monitoring, by flushing the sand from the PVC casing using high-pressured drilling mud.

The associated earth station and batteries were buried behind a concrete barrier along the shoulder of the highway. This station houses the earthquake alarm, which serves to wake up the array if the acceleration reading of this surface-mounted accelerometer exceeds a prescribed threshold. The threshold was set at 0.03 g and can be changed remotely via the FTP server. Maximum reading of the earthquake sensor for the first six months of monitoring was 0.002 g. The FTP server also receives all the data from the SAA at prescribed intervals via a wireless modem in the earth station.

Fig. 17 presents a comparison of the SAA and traditional inclinometer displacement readings, for an eighteen month period of monitoring. For both the SAA and the inclinometer casing, the x-direction and A-axis, respectively, were oriented in the anticipated direction of primary displacement, i.e. downslope. Cumulative displacements remain less than 20.0 mm for both measurement systems, but the general trends are visible and comparable. Since the SAA and the inclinometer casing were located about one meter apart and the SAA casing was backfilled with sand, the displacement values are not expected to be exactly the same. The observed differences can likely be attributed to the settling of the sand backfill between the SAA and the 76 mm casing. It is also possible that there is a depth positioning discrepancy between the systems as the inclinometer and SAA data profiles would nearly align if the inclinometer data was shifted down by 0.6 m, or the length of the inclinometer probe.

For the dry summer season, the “Site A” array was set to upload tilt, vibration, and temperature data to the FTP server once a week, after an initial checkout period during which data are sent several times a day. This uploading interval can be adjusted remotely and was changed to once a day in November 2006, in anticipation of a rainy winter season. Site preparation and drilling at this site took approximately three and a half hours, installation of the PVC casing and SAA took two hours, and installation of the earth station

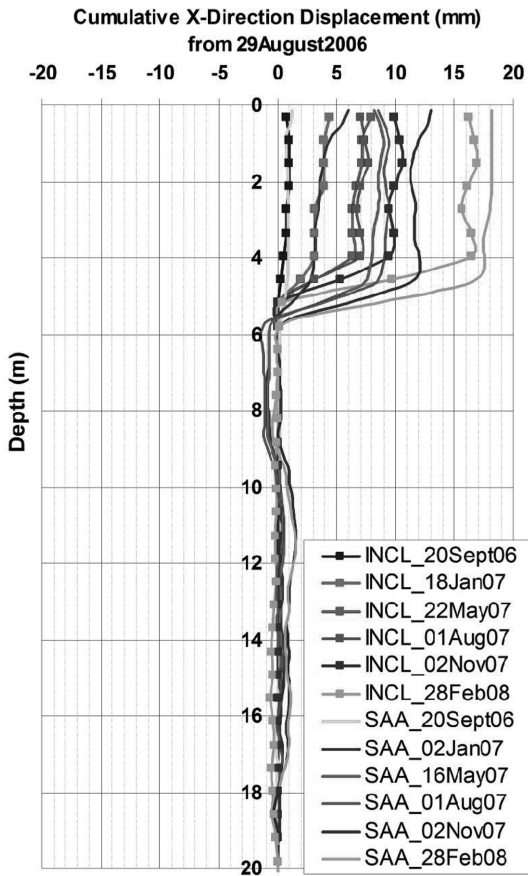


Fig. 17 Comparison between a traditional inclinometer reading (lines with markers) and the wireless ShapeAccelArray system (lines without markers) reading of x-direction displacement for an eighteen month period at “Site A”, California

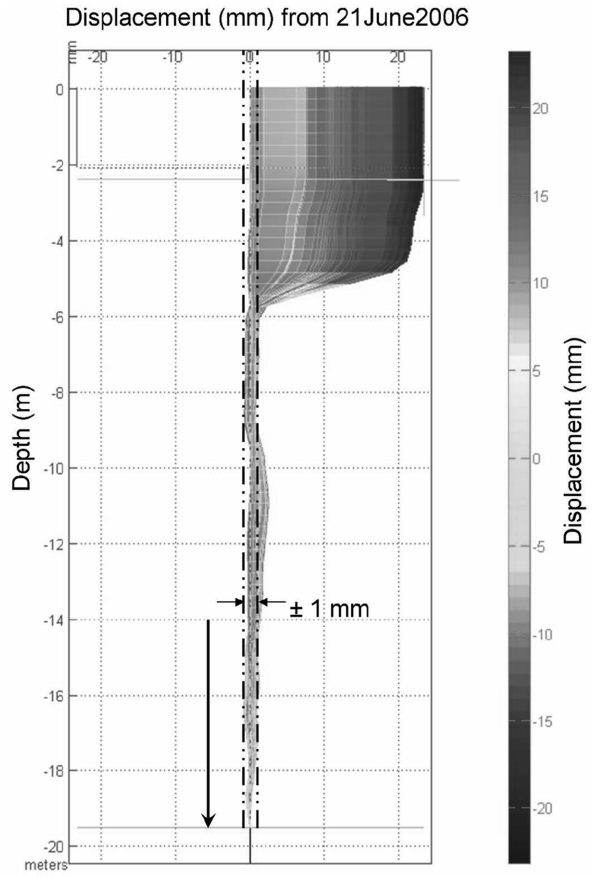


Fig. 18 Wireless ShapeAccelArray system stability in stable soil layer over a two-year monitoring period, “Site A”, California

took one and a half hours. The first data sets were uploaded to the FTP server by wireless cellnet modem within a few minutes of connection of the earth station to the SAA.

The accuracy of the deformation measurement of the SAA is +/-1.5 mm per 30 m. The SAA system accuracy specification was derived empirically from thousands of datasets over a period of two years, from three different field locations. Fig. 18 presents a maximum displacement fluctuation of ± 1.0 mm in the known stable soil layer below 14 m depth, over a two year monitoring period at “Site A”.

7. Conclusions

Measured lab and field data indicate that MEMS-based in-place inclinometer systems can be used successfully to measure 3D permanent displacements and accelerations as part of a geotechnical monitoring program. Small- and large-scale laboratory tests show favorable comparisons between

measurements from the MEMS-based system and traditional methods of instrumentation. However, this MEMS-based system is only able to capture the permanent lateral displacement during an earthquake event, as indicated by the full-scale validation tests. The California field test was an excellent trial opportunity for the MEMS-based system and also showed favorable displacement comparisons between the MEMS-based data and traditional probe inclinometer data. These preliminary results demonstrate that the above algorithms work with the MEMS devices to simultaneously and accurately measure acceleration and permanent ground displacement in situ. The field installations addressed some of the questions surrounding the use of MEMS devices in geotechnical instrumentation and furthered confidence in the temperature calibration of this system. The successful monitoring at the site described above and several others is ongoing and the data confirms the system accuracy (± 1.5 mm per 30 m) to be comparable to conventional probe inclinometers, but with improved spatial resolution (readings at 0.305 m increments).

Acknowledgements

This research is supported by the NSF sensor program; this support is gratefully appreciated. The authors would also like to express their sincere thanks to Prof. M. Symans and Dr. D. Reigles of Rensselaer Polytechnic Institute and Dr. N. Ecemis and Mr. M. Pitman of the University at Buffalo NEES equipment site for their help in conducting the 1g shaking table tests and 1g laminar container tests. The authors would also like to express their gratitude to the Caltrans engineers, drillers and maintenance staff who participated in these field installations.

References

- Abdoun, T., Danisch, L., Ha, D. and Bennett, V. (2006), "Advanced sensing for real-time monitoring of geotechnical systems", *Transportation Research Board (TRB) 85th Annual Meeting*, Washington, D.C., January 22-26.
- Abdoun, T., Bennett, V., Danisch, L., Shantz, T. and Jang, D. (2007), "Field installation details of a wireless shape-acceleration array system for geotechnical applications", *Proc. of SPIE*, San Diego, CA, March 19-22, Vol. 6529.
- Danisch, L.A. (1998), *Fiber optic bending and positioning sensor*, PCT 0,702,780, International PCT patent.
- Danisch, L.A., Danisch, J.F. and Lutes, J. (2003), *Topological and motion measuring tool II (ShapeRope)*, US Patent Notice of Issue.
- Danisch, L.A., Lowery-Simpson, M.S. and Abdoun, T. (2004), *Shape-Acceleration measurement Device and Method*, Patent Application.
- Elgamal, A.W., Zeghal, M., Tang, H.T. and Stepp, J.C. (1995), "Lotung downhole seismic array: evaluation of site dynamic properties", *J. Geotech. Eng. ASCE*, **121**(4), 350-362.
- Elgamal, A.W., Zeghal, M. and Parra, E. (1996), "Liquefaction of an artificial island in kobe, japan", *J. Geotech. Eng. ASCE*, **122**(1).
- Hoffman, K., Varuso, R. and Fratta, D. (2006), "The use of low-cost MEMS accelerometers in near-surface travel-time tomography", *Proc. of GeoCongress 2006 Conf.*, Atlanta, GA.
- Lynch, J.P., Law, K.H., Kiremidjian, A.S., Carryer, E., Farrar, C.R., Sohn, H., Allen, D., Nadler, B. and Wait, J. (2004), "Design and performance validation of a wireless sensing unit for structural monitoring applications", *Struct. Eng. Mech.*, **17**(3).
- Pakzad, S.N. and Fennes, G.L. (2004), "Structural health monitoring applications using MEMS sensor networks", *4th Int. Workshop on Structural Control*, Columbia University, June 10-11, 47-56.
- Reigles, D. (2005), "Smart base isolation systems for seismic response control of plan-asymmetric buildings",

- Ph.D. Dissertation, Rensselaer Polytechnic Institute, Troy, NY.
- Sellers, B. and Taylor, R. (2008), "MEMS basics", *Geotechnical News Magazine*, **26**(1), 32-33.
- Tanner, N., Wait, J., Farrar, C. and Sohn, H. (2003), "Structural health monitoring using modular wireless sensors", *J. Intel. Mat. Syst. Str.*, **14**(1), 43-56.
- Youd, T.L. and Holzer, T. (1994), "Piezometer performance at wildlife liquefaction site, california", *J. Geotech. Eng. ASCE*, **120**(6), 975-995.
- Zeghal, M. and Elgamal, A.W. (1994), "Analysis of site liquefaction using earthquake records", *Geotech. Eng. ASCE*, **120**(6), 996-1017.
- Zeghal, M., Elgamal, A.W., Tang, H.T. and Stepp, J.C. (1995), "Lotung downhole seismic array: evaluation of soil nonlinear properties", *J. Geotech. Eng. ASCE*, **121**(4), 363-378.

BS